The Astrophysical Journal, 763:103 (7pp), 2013 February 1 doi:10.1088/0004-637X/763/2/103

SEMIREGULAR VARIABLES WITH PERIODS LYING BETWEEN THE PERIOD–LUMINOSITY SEQUENCES C′, C, AND D

I. Soszyński[1] and P. R. Wood[2]
[1] Warsaw University Observatory, Al. Ujazdowskie 4, 00-478 Warszawa, Poland; soszynsk@astrouw.edu.pl
[2] Research School of Astronomy and Astrophysics, Australian National University, Cotter Road, Weston Creek, ACT 2611, Australia; wood@mso.anu.edu.au
Received 2012 October 18; accepted 2012 December 1; published 2013 January 15

ABSTRACT

We analyze the distribution of semiregular variables and Mira stars in the period–luminosity plane. Our sample consists of 6169 oxygen-rich long-period variables in the Large Magellanic Cloud included in the OGLE-III Catalog of Variable Stars. There are many stars with periods that lie between the well-known sequences C and C′. Most of these stars are multi-periodic and the period ratios suggest that these stars oscillate in the same mode as the sequence C stars. Models suggest that this mode is the fundamental radial pulsation mode. The stars with primary periods between sequences C and C′ preferentially lie on an additional sequence (named F), and a large fraction of these stars also have long secondary periods (LSPs) that lie between sequences C and D. There are also a small number of stars with primary periods lying between sequences C and D. The origin of this long-period variability is unknown, as is the cause of sequence D variability. In addition, the origin of sequence F is unknown but we speculate that sequence F variability may be excited by the same phenomenon that causes the LSPs.

Key words: infrared: stars – stars: AGB and post-AGB – stars: late-type – stars: oscillations (including pulsations)

Online-only material: color figures

1. INTRODUCTION

Variability of red giant stars is one of the least understood aspects of stellar astrophysics. It is known that all stars in the upper part of the first ascent red giant branch (RGB) and on the asymptotic giant branch (AGB) vary, and the amplitude of variation tends to increase toward higher bolometric luminosity. Traditionally, long-period variables (LPVs) have been divided into three types: Miras, semiregular variables (SRVs), and irregular variables (see the General Catalog of Variable Stars, GCVS; Kholopov et al. 1985–1988). The existence of irregular variables (i.e., variable stars with no sign of periodicity) among red giants is in dispute (Kerschbaum et al. 2001; Lebzelter & Obbrugger 2009). On the other hand, a very numerous group of pulsating red giants, called OGLE Small Amplitude Red Giants (OSARGs; Wray et al. 2004), seem to constitute a separate class of variable red giant, different from Miras and SRVs (Soszyński et al. 2004a).

In the classical picture, semiregular red giants are subclassified into SRa and SRb stars. The definitions provided in the GCVS do not give strict criteria to distinguish between both subtypes. SRa stars display persistent periodicities with variable amplitudes and light curve shapes, while SRb stars have poorly defined periodicities or show alternating intervals of periodic and slow irregular changes. So far, it has not been clear whether both types form a continuum or represent distinct classes of LPVs.

In recent years, our knowledge of the distribution of LPVs in the period–luminosity (PL) plane has significantly expanded. Before the era of large microlensing surveys, two PL relations obeyed by LPVs at near-infrared (NIR) wavelengths were known: one discovered by Glass & Lloyd Evans (1981) for Mira stars and the second noticed by Wood & Sebo (1996) for SRVs. The long-term, massive photometry obtained by the microlensing projects (MACHO; Optical Gravitational Lensing Experiment, OGLE; EROS) together with observations from the large-scale NIR surveys (e.g., Two Micron All Sky Survey, 2MASS; DENIS; IRSF) showed a very complex pattern formed by LPVs in the PL plane. Wood et al. (1999) and Wood (2000) distinguished and labeled with letters A–E five PL ridges. Later studies (Kiss & Bedding 2003; Ita et al. 2004; Soszyński et al. 2004a, 2005, 2007; Fraser et al. 2008) increased to 14 the number of known PL relations obeyed by LPVs when separate sequences are assigned to C stars and O-rich stars, and to AGB and RGB stars (see Table 1 in Soszyński et al. 2007). Furthermore, some of these sequences, especially sequences A and B, appear to be split into two or three close parallel sequences.

Figure 1 presents the PL diagram for LPVs in the Large Magellanic Cloud (LMC). The data originate from the OGLE-III Catalog of Variable Stars[3] (OIII-CVS; Soszyński et al. 2009). Using the notation introduced by Wood et al. (1999) and other authors, Miras belong to sequence C, while SRVs occupy sequences C and C′. OSARG variables populate sequences A and B, and several additional ridges (Soszyński et al. 2004a). The OSARG variables on the RGB and on the AGB follow somewhat different sets of PL relations, shifted in period relative to each other (Kiss & Bedding 2003). Sequence D corresponds to the long secondary periods (LSPs)—a still unexplained phenomenon existing in at least one-third of SRVs and OSARGs (e.g., Wood et al. 2004; Nicholls et al. 2009). Sequence E consists of eclipsing or ellipsoidal close binary systems with a red giant as one of the components (Wood et al. 1999; Soszyński et al. 2004b; Nicholls et al. 2010).

Soszyński et al. (2005) noticed an additional PL ridge spreading between sequences C and C′. This new PL relation is obeyed by SRVs with relatively small amplitudes. The existence of this additional sequence was confirmed for rich samples of LPVs in the LMC (Soszyński et al. 2009) and Small Magellanic Cloud (Soszyński et al. 2011). Here, we analyze in detail red

[3] The catalog data are publicly available from the FTP site ftp://ftp.astrouw.edu.pl/ogle/ogle3/OIII-CVS/lmc/lpv/ or via the Web site http://ogledb.astrouw.edu.pl/~ogle/CVS/.

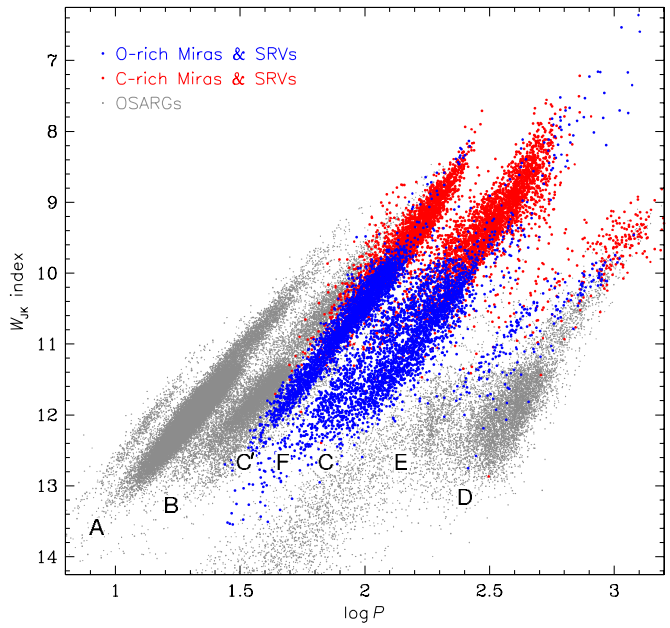

Figure 1. Period–luminosity diagram for LPVs in the LMC. Each star is represented by one point, corresponding to the primary (dominant) period. Different colors refer to different types of variable sources: blue points are O-rich SRVs and Miras, red points indicate C-rich SRVs and Miras, and gray points show OSARG variables. Periods used for the sequence E stars (binary systems) are half of the orbital periods. Periods and classification of stars were taken from the OGLE-III Catalog of Variable Stars (Soszyński et al. 2009), while J and K magnitudes used to construct the Wesenheit index originate from the 2MASS All-Sky Point Source Catalog (Cutri et al. 2003).

giants lying on this sequence and generally between sequences C and C′.

2. OBSERVATIONAL DATA

In this work, we restrict our analysis to the sample of LPVs in the LMC, since this galaxy hosts very large numbers of AGB stars with well-defined multiple PL relations. The collection of LPVs was extracted from the OIII-CVS (Soszyński et al. 2009). The light curves published in the catalog were obtained with the 1.3 m Warsaw telescope at Las Campanas Observatory, Chile, over the period 2001 June–2009 May (the time span of the OGLE-III survey). The telescope and the instrumentation are described in detail by Udalski (2003). For stars in the central part of the LMC, the OGLE-II observations obtained from 1997 January to 2000 November were also included. About 90% of the OGLE photometric measurements were collected in the Cousins I band, and we used these data to analyze periodicities and amplitudes of our sample. Here, we concentrate on the oxygen-rich (O-rich) SRVs and Miras. Note that we have adopted the definition of SRVs and Miras given by Soszyński et al. (2007): they have periods located on sequences C and/or C′ but do not have periods on any of the shorter period sequences (stars with periods on any of the shorter period sequences are designated as OSARG variables). We decided not to include carbon-rich (C-rich) LPVs, because they occupy the upper part of the PL diagram (Figure 1) and sequence F is most easily distinguishable for the fainter O-rich stars.

The OGLE catalog of LPVs in the LMC contains in total 6445 O-rich SRVs and Miras. In the present analysis, we re-derived periods provided in the catalog, with the iterative procedure of fitting and subtracting the irregular slow variations. We used the FNPEAKS code by Z. Kołaczkowski, which is based on Fourier analysis. For each object, we found the three most significant periods. All light curves folded with the primary (largest amplitude) periods were visually inspected and, in some cases, the periods were judged to be spurious and were replaced by one of the additional periodicities. The additional periods were not inspected and in some individual cases they may be spurious, although the statistical properties of the sample should still be visible with these automatically derived periods. The peak-to-peak amplitudes $A(I)$ were derived by fitting a third-order Fourier series to the detrended I-band light curves. Following Soszyński et al. (2009), we define Mira stars as those having I-band amplitudes larger than 0.8 mag, although we did not note any clear natural boundary between O-rich Miras and SRVs, as found for C-rich LPVs by Soszyński et al. (2009). We were left with 5712 SRVs and 457 Miras (96% of the initial sample) with relatively well-defined primary periods. For over 90% of stars in our sample, we obtained practically the same (differing by less than 2%) primary periods as provided in the OIII-CVS.

NIR J and K_s measurements of the stars were obtained from the 2MASS All-Sky Point Source Catalog (Cutri et al. 2003). To avoid the effects of interstellar and circumstellar extinction, we constructed the reddening-free Wesenheit index, defined as

$$W_{\rm JK} = K_s - 0.686(J - K_s),$$

where the coefficient $0.686 = A_K/E(J-K)$ was derived assuming the extinction law provided by Schlegel et al. (1998). The distribution of LPVs in the period–$W_{\rm JK}$ plane is very similar to the distribution in the period–K_s plane, with the exception of LPVs with heavy circumstellar extinction (usually C-rich Miras, e.g., Ita & Matsunaga 2011), which show significantly lower brightness in the K_s band than expected from a linear extension of the period–K_s relation.

3. RESULTS AND DISCUSSION

3.1. The Amplitudes and Shapes of the Light Curves

The goal of our study is to learn more about SRVs lying between sequences C and C′. The sample of stars we examined was delimited in the log P–$W_{\rm JK}$ diagram by the two lines of slope $dW_{\rm JK}/d\log P = 4.444$ which are shown in panel (a) of Figure 2. Panel (b) of Figure 2 shows the histogram of the number of stars horizontally across the strip between the two lines in panel (a). We use the parameter $\log P(W_{\rm JK} = 12)$ to measure the horizontal position of a point, where $\log P(W_{\rm JK} = 12)$ is the value of $\log P$ obtained by projecting a star's true $\log P$ down or up to $W_{\rm JK} = 12$ along a line parallel to those shown in panel a of Figure 2. There are two peaks in this histogram, one with $\log P(W_{\rm JK} = 12) \approx 1.95$ which corresponds to sequence C, and a second weaker peak at $\log P(W_{\rm JK} = 12) \approx 1.82$. Hereafter, we refer to this ridge as sequence F, since F is the next letter (in alphabetical order) after the series of designations introduced by Wood et al. (1999).[4]

The amplitudes of our sample of stars are plotted against $W_{\rm JK}$ and $\log P(W_{\rm JK} = 12)$ in panels (c) and (d) of Figure 2, respectively. Panel (d) shows that the amplitude of variation

[4] Ita et al. (2004) used label F to designate the PL relation for classical Cepheids, but we propose to continue this naming scheme only for red giant stars.

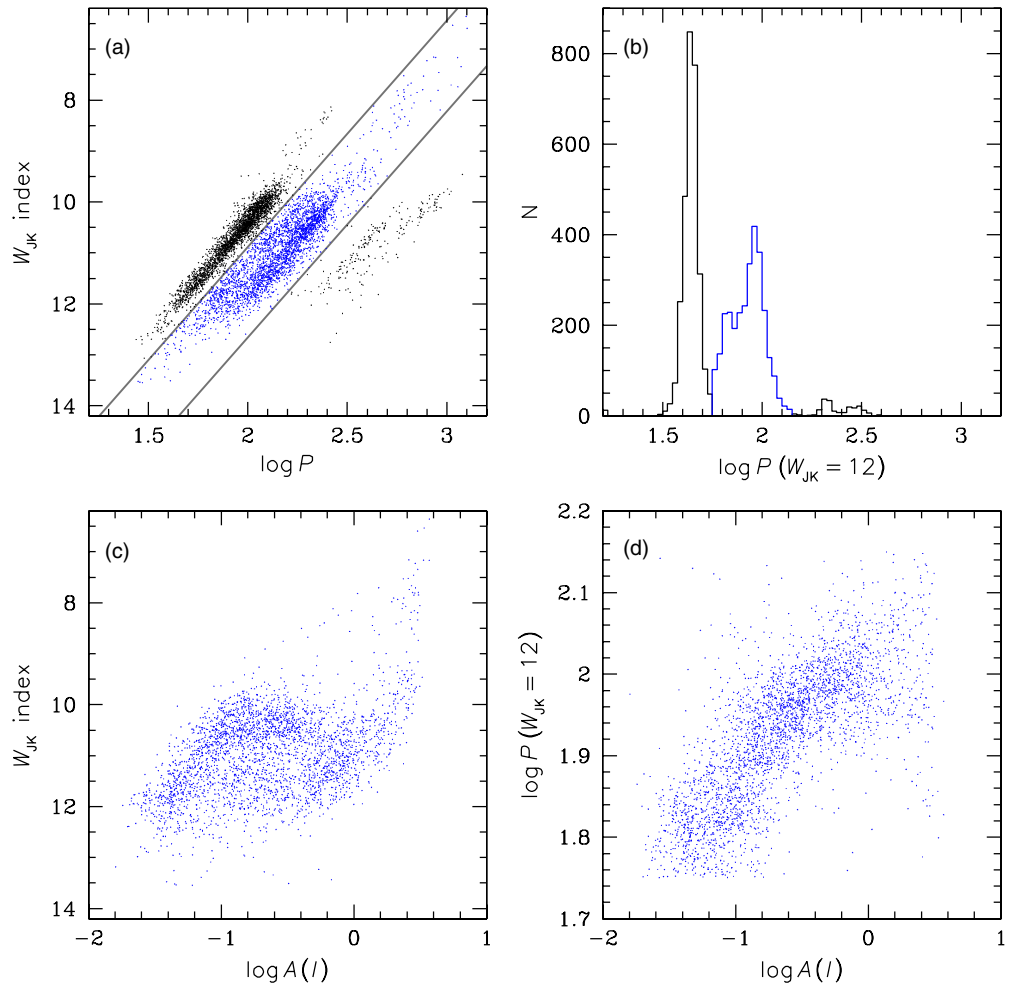

Figure 2. (a) The W_{JK}–log P diagram for the O-rich SRVs and Miras in this study, where P is the primary period of variation. The two diagonal lines form the boundary of the region occupied by stars between sequences C′ and C. (b) The histogram of the number of stars as a function of log $P(W_{JK} = 12)$, where log $P(W_{JK} = 12)$ is the value of log P obtained by projecting a star's true log P to $W_{JK} = 12$ along a line parallel to those shown in panel a. (c) The W_{JK}–log $A(I)$ plot for the stars between the two diagonal lines in panel (a), where $A(I)$ is the full I amplitude of the primary period of variation. (d) The log $P(W_{JK} = 12)$–log $A(I)$ diagram for these stars. (A color version of this figure is available in the online journal.)

increases steadily with log $P(W_{JK} = 12)$, corresponding to movement from sequence F to sequence C. The two sequences F and C can be clearly seen in panel (c), where the sequence F stars lie near the low-amplitude edge of the populated region while the sequence C stars lie near the high-amplitude edge. At brighter luminosities ($W_{JK} \sim 10.5$), the amplitudes of the sequence F stars appear to increase toward the amplitudes typical of sequence C stars. These stars are possibly at the stage of increasing their surface carbon abundance and will soon evolve into carbon-rich variables of sequence C (the carbon stars merge with the O-rich stars at $W_{JK} \sim 10$).

Although the exact correspondence between the stars studied here and the classical designations SRa and SRb is unclear, the smaller amplitudes of the sequence F stars suggest that they may belong to the SRb class while the sequence C stars belong to the SRa class. Several example light curves of stars from the two sequences are shown in Figure 3. The larger-amplitude sequence C variables are Miras or SRVs with well-defined periods, so they can readily be classified as Mira and SRa stars. The lower-amplitude sequence F stars generally have much more poorly expressed periodicity, with strong irregular components in the light curves, characteristics typical of SRb stars.

3.2. The Nature of the Variable Stars between Sequences C′ and C

In order to understand the nature of the variable stars between sequences C′ and C, we compare observations with models in Figure 4. In particular, we examine the belief that the cause of variability in these stars is predominantly due to pulsation in radial modes[5] (Wood & Sebo 1996; Wood et al. 1999; Soszyński et al. 2007). The linear, non-adiabatic, radial pulsation models used here were constructed with the code described by Fox & Wood (1982) and updated by Keller & Wood (2006). An additional update for the current models is the use of opacities from Marigo & Aringer (2009) which include a molecular

[5] We note that *CoRoT* (e.g., Mosser et al. 2010) and *Kepler* (e.g., Kallinger et al. 2010) observations of red giants about one order of magnitude fainter than our sample are yielding data on many convectively excited radial and non-radial modes. At this stage, differential frequency or period information from the space-based observations are being used to derive information about the global and interior properties of the stars. The actual radial order of the modes is not precisely known. The present study of the most luminous giants aims to model the values of the periods of known radial modes in terms of global stellar properties. As the space-based observation sequences become longer and the luminosities of the red giants with detected frequencies begin to overlap with the giants observed by OGLE, we can expect a merger of these two approaches.

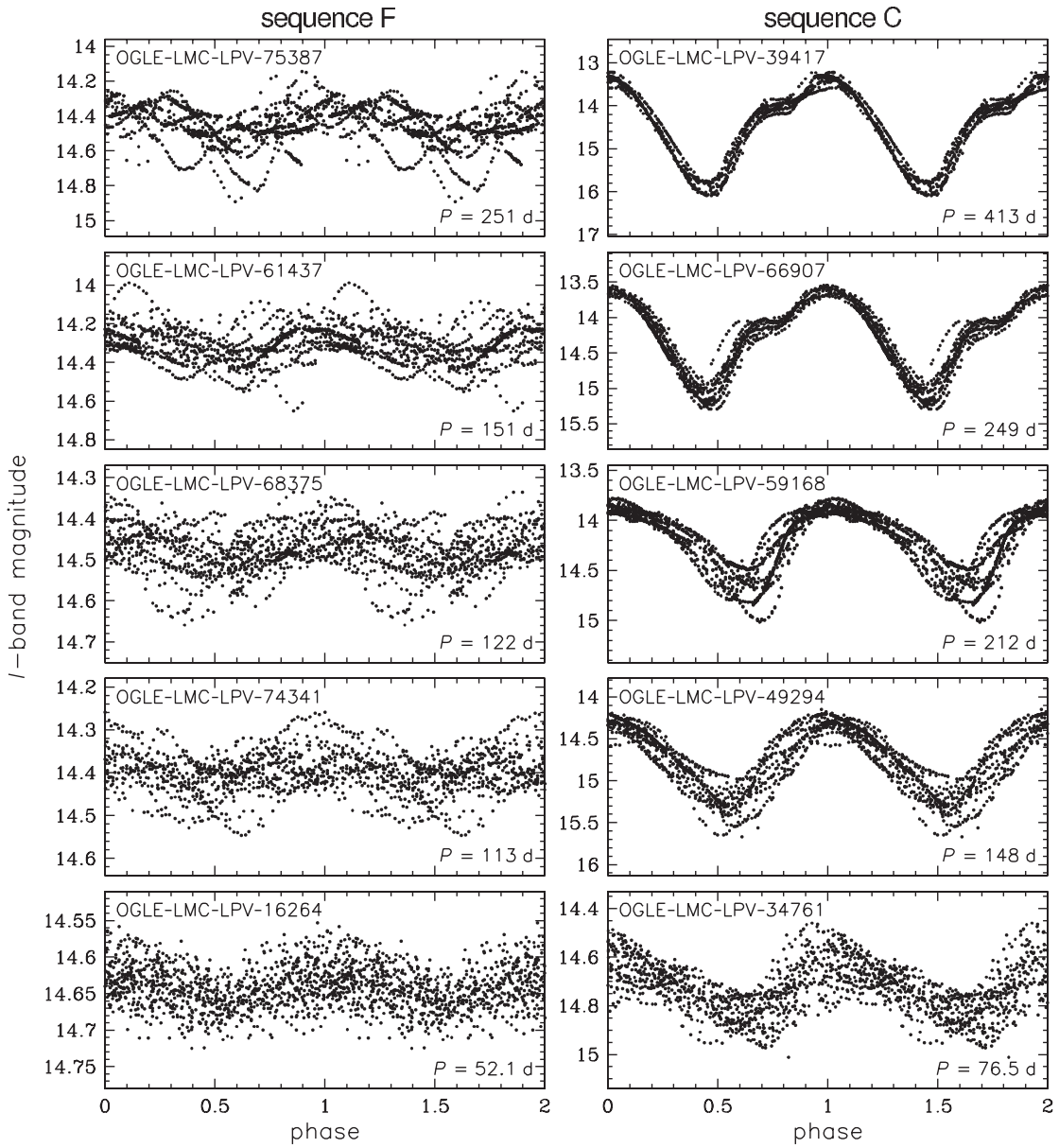

Figure 3. Example *I*-band light curves of SRVs with the primary periods lying on PL sequence F (left panels) and SRV/Mira stars which populate sequence C (right panels). The light curves are folded with the periods given in each panel.

component in the outer layers. The models use a composition $Y = 0.73$ and $Z = 0.008$, a mixing length of 1.97 pressure scale heights (to reproduce the giant branch temperature given by Kamath et al. 2010 for the luminous O-rich stars in the populous intermediate-age cluster NGC 1978) and a turbulent viscosity parameter $\alpha_v = 0.25$.

The top panel of Figure 4 shows the observed stars in the W_{JK}–log P diagram. Also shown are the positions occupied by 0.9 $M_\odot$ stars pulsating in the fundamental and first overtone modes. The models have been adjusted to the LMC using the distance modulus 18.54 mag and reddening $E(B-V) =$ 0.08 mag given by Keller & Wood (2006).

The first thing to note about this diagram is that the lines corresponding to a fixed mode and a fixed mass are not parallel to the observed sequences. A given star will evolve along these lines (neglecting mass loss, which should be a minor effect for these optically visible stars). The observed variability sequences are defined by the positions on these lines at which the mode is unstable, and by the range of mass values in the stellar population being considered (higher mass stars have tracks to the left of, or equivalently above, the lines shown, and vice versa for lower mass stars).

The computed stability of the modes in red giant stars is very uncertain due to the fact that convection carries most of the flux through most of the envelope and our knowledge of the transport of energy by convection is poor (the mixing-length theory of convection is used here). Nevertheless, the computed growth rates (middle panel of Figure 4) qualitatively confirm the above picture. It can be seen that the peak in the growth rate for the first overtone mode occurs at the periods where the black line crosses sequence C′, as required. The fundamental mode only becomes unstable at the highest luminosities, again consistent with observations. However, in the models, the fundamental mode becomes unstable at the long-period edge of sequence C rather than on the short-period edge. This is clearly a quantitative deficiency in the models. Note that the right-hand edge of sequence C is defined not by the fundamental mode becoming stable again, but by loss of the stellar envelope caused by large-

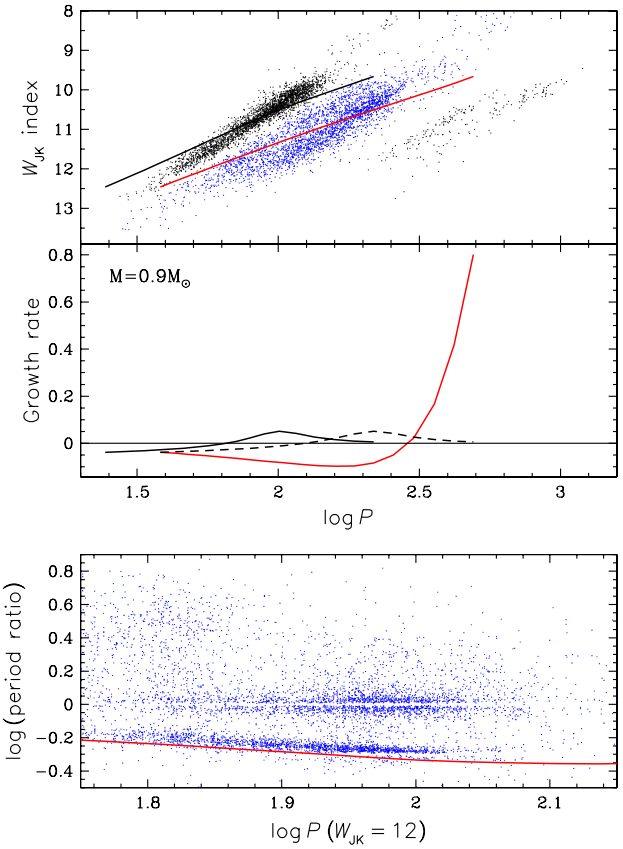

Figure 4. Top panel: the W_{JK}–log P diagram on which are superimposed the positions of 0.9 $M_\odot$ radial pulsation models for the fundamental mode (red; black in the print journal) and the first overtone (black; grey in the print journal). Middle panel: the growth rates (fractional increase in amplitude per period) for the fundamental radial pulsation mode (red; black in the print journal) and the first overtone radial pulsation mode (black; grey in the print journal). The solid lines show the growth rate plotted against the mode period while the dashed line shows the first overtone growth rate plotted against the fundamental mode period (thus points on the red line (black line in the print journal) and the dashed black line (grey line in the print journal) with the same period correspond to the same luminosity and model). Bottom panel: the period ratios P_2/P_1 and P_3/P_1 plotted against log $P_1(W_{JK} = 12)$, where P_1 is the primary observed period of variation and P_2 and P_3 are the secondary and tertiary observed periods. Also shown is the ratio of the first overtone period to the fundamental mode period for the 0.9 $M_\odot$ models plotted against log $P(W_{JK} = 12)$ for the fundamental mode (red line; black line in the print journal).

(A color version of this figure is available in the online journal.)

amplitude Mira-like pulsation. This general pattern of modal instability and mass loss has been described before by Wood et al. (1983) and Vassiliadis & Wood (1993).

Using the above picture, the evolution of AGB stars can be described qualitatively as follows. A 0.9 $M_\odot$ star evolving up the AGB will (neglecting helium shell flashes) move to higher luminosities until its first overtone mode becomes unstable, at which time it will belong to the left side of sequence C′. With further evolution, the star will move to higher luminosities and through to the right side of sequence C′. The growth rates shown in Figure 4 suggest that the growth rate, and presumably the amplitude of pulsation, will be less there than when the star was near the center of sequence C′. Eventually, the star will become unstable in the fundamental mode and the fundamental mode will become dominant. At this stage, the star will make a transition to sequence C at constant luminosity.

Exactly how this transition occurs is quite uncertain. The growth rates shown in Figure 4 suggest that the first overtone remains unstable when the fundamental mode becomes unstable, suggesting that both modes will be active simultaneously at certain luminosities (the red (black in the print journal) and dashed curves in Figure 4 should be used to compare the growth rates in the same star). However, the computed growth rates are very uncertain and, in particular, the (totally unknown) values of the turbulent viscosity parameter α_ν can be used to suppress the growth rates by varying amounts. It is even possible that after the star has evolved through the region where the first overtone is unstable, both this mode and the fundamental mode will be stable over a small luminosity interval. In this case, any modes that are seen would be excited externally, for example by convective motions or some other mechanism. This possibility is discussed more in the next subsection.

The bottom panel of Figure 4 plots the period ratios P_2/P_1 and P_3/P_1 against log $P_1(W_{JK} = 12)$ (we remind the reader that up to three periods were determined for each star, with the primary period P_1 corresponding to the largest-amplitude period). Note that the range of log $P_1(W_{JK} = 12)$ shown corresponds to the complete width of the region containing sequences F and C (the blue points (black points in the print journal) in the top panel). We will hereafter designate stars with $1.75 < \log P_1(W_{JK} = 12) < 1.9$ as sequence F stars and stars with $1.9 < \log P_1(W_{JK} = 12) < 2.15$ as sequence C stars. The empty strip in the bottom panel of Figure 4 at log(period ratio) = 0.0 is the zone where additional modes are unresolvable for the current length of the OGLE data series. Similar empty strips occur at period ratios of 1/2 and 1/3 since each period is fitted by the primary frequency and two harmonics. Points with $-0.1 \lesssim \log(P_2/P_1) \lesssim 0.1$ or $-0.1 \lesssim \log(P_3/P_1) \lesssim 0.1$ presumably correspond to multiple detections of the same mode. It is well known that the periods of LPVs vary erratically (e.g., see Figure 10 of Wood et al. 2004 or Templeton et al. 2005) so that the same mode may be detected by Fourier analysis multiple times due to period variability.

There is a well-defined locus of points on a line with $-0.3 \lesssim \log(P/P_1) \lesssim -0.15$ corresponding to the simultaneous existence of two modes. The red line (black line in the print journal) in Figure 4 shows the ratio of the first overtone period to the fundamental mode period. This line follows the general shape of the observed locus of points (although offset by a small amount, indicating that the structure of red giant models constructed using the mixing-length theory of convection and extant opacities is not a good match to the structure of real stars). It seems clear from the near-coincidence of the models and observations that all of the points on the observed locus correspond to stars in which both the fundamental and first overtone radial modes are active. The lack of a corresponding locus of points at positive values of $\log(P/P_1)$ shows that the fundamental mode oscillation dominates the first overtone oscillation for sequence F stars as well as for sequence C stars, i.e., P_1 in these stars is the fundamental radial mode. The fraction of sequence C stars with a detected first overtone pulsation is 49% and the fraction of sequence F stars with a detected first overtone pulsation is 56%. It is therefore reasonable to assume that all the stars on sequences F and C are fundamental mode pulsators.

The above analysis does not give any reason for expecting a second sequence for fundamental mode pulsation i.e., sequence F in addition to sequence C, as suggested by the histogram in panel (b) of Figure 2. One possible way to produce sequence F

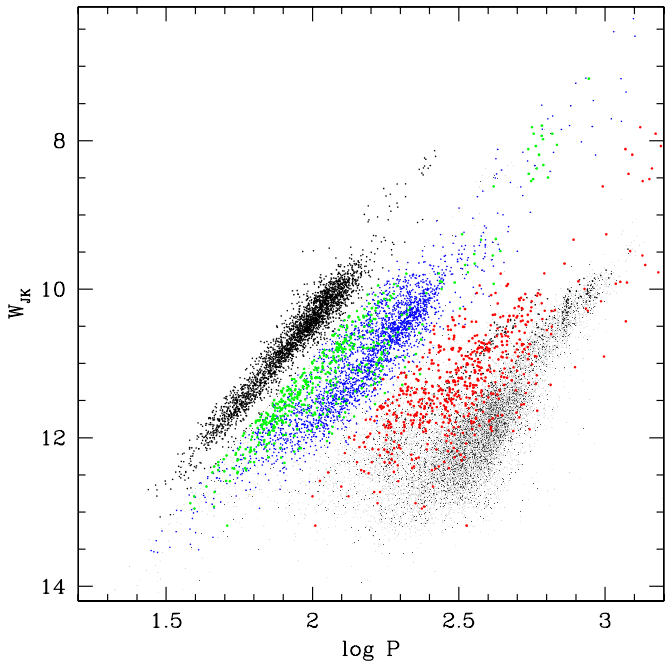

Figure 5. W_{JK}–log P diagram for the O-rich SRVs and Miras in this study, where P is the primary period of variation. Blue points are stars with their primary pulsation periods on sequences F or C. Green points are sequence F or C stars that also have an additional period longer than sequence C, where these additional periods are shown as red points. The black points are stars whose primary periods lie on sequence C′ or stars with primary periods longer than the sequence C periods. The faint gray points are all the OSARG variables from the OGLE III catalog of LPVs that have a primary period longer than sequence C. They are plotted to show the position of sequence D.

would be to have a positive bump in the growth rate of the fundamental mode near $\log P \sim 2$ in the middle panel of Figure 4. However, in our models, the growth rate behaves smoothly with $\log P$, so the present models cannot explain sequence F in this way.

3.3. Long Secondary Periods in Sequence F Stars

A notable feature in the bottom panel of Figure 4 is the considerable fraction (33%) of sequence F stars in which P_2 or P_3 is an LSP with $\log(P/P_1) > 0.3$. A much smaller fraction (8%) of sequence C stars have LSPs defined in this way.

Figure 5 shows the positions of the LSPs associated with sequence F and C stars as red points in the W_{JK}–log P diagram. The stars on sequences F or C that host these LSPs are marked as green points. It is clear from Figure 5 that the LSPs lie predominantly between sequence C and sequence D. Note that there is also a small number of variables that have their primary periods in this region (see Figure 1, Figure 5 or panel (a) of Figure 2). These stars seem to fall on a quite tight sequence and some examples of their light curves are shown in Figure 6. We do not know the origin of either the primary periods or the LSPs that lie between sequences C and D (nor do we understand the origin of the LSPs associated with sequence D—see Wood et al. 2004; Nicholls et al. 2009). The concentration of green points on sequence F suggests that there is some relation between the sequence F fundamental mode oscillations and the LSPs lying between sequences C and D. Perhaps the LSPs excite the fundamental mode pulsation seen on sequence F.

It is very notable that the ratio of the LSP to the fundamental mode period is not precisely defined, in contrast to the ratio of first overtone period to the fundamental mode period (see the

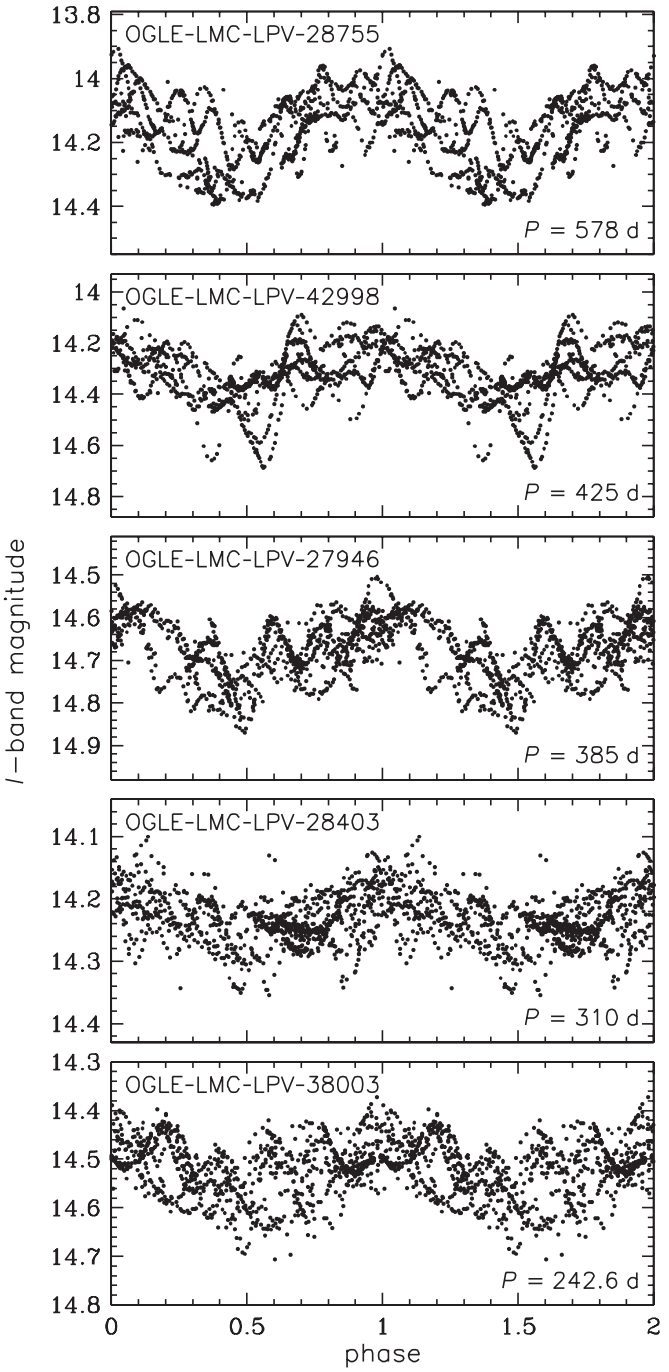

Figure 6. Example I-band light curves of stars with the primary periods falling between sequences C and D. The light curves are folded with the periods given in the panels.

bottom panel of Figure 4). This suggests that the LSPs are not caused by one (or a few) pulsation modes. Some completely separate mechanism must be involved.

In their study of 247 red giants in the solar neighborhood, Tabur et al. (2010) reported the discovery of LPVs with periods falling between sequences C and D. They attributed these periodicities to the stellar noise from convection. However, this is not the only possible explanation of the physical origin of these periods. Another possible explanation assumes that these are binary systems, since these objects are on the extension of sequence E populated by ellipsoidal and eclipsing binaries. In such a case, their orbital periods should be two times

longer than the photometric period shown in the PL diagram (Soszyński et al. 2004b; Nicholls et al. 2010). However, their light curves do not exhibit characteristic features of ellipsoidal or eclipsing variables (alternating deep and shallow minima and/or eclipses). Figure 6 shows an example set of the light curves folded with the photometric periods falling between sequences C and D. Although ellipsoidal modulation is not excluded, there is no clear evidence for binarity as seen in the case of the sequence E stars. Other possible non-pulsating explanations for the periods that lie between sequences C and D are rotation of a spotted star and star spot cycles (Wood et al. 2004) and a long-period convective cycle (Stothers 2010). It is possible that the same physical mechanism applies to all of the stars with periods longer than sequence C, whether these periods lie on sequence D or between sequences C and D.

4. CONCLUSIONS

We have examined the distribution of SRVs and Mira variables in the W_{JK}–log P diagram. These stars all have periods on, or longer than, those of sequence C′. Although the majority of variables have periods on the well-known sequences C and C′, many variables lie between sequences C and C′ and a small number have primary periods between sequences C and D. There appears to be a concentration of stars on a faint sequence roughly halfway between sequences C and C′: we label this sequence F. These stars have small amplitudes, approximately 0.1 times those of stars on sequence C, and poorly defined periodicity so they would be defined as SRb variables in the classical subdivisions of LPVs given in the GCVS. For variables between sequences C′ and C, there is a general increase in amplitude with luminosity and with increasing period while at constant luminosity. Many of the stars with primary periods on sequence F have secondary periods lying between sequences C and D.

Most of the stars with primary periods lying between sequences C and C′ are multimode variables. Comparison of the period ratios in these stars with theoretical pulsation models shows that the primary period is the period of the fundamental mode of radial pulsation. Approximately 50% of the stars have detected pulsations in the first overtone mode. The growth rates in the models qualitatively predict the existence of sequences C and C′, these being the regions of instability of the fundamental and first overtone modes, respectively. However, there is no evidence in the models for an increase in the growth rate in the vicinity of sequence F. We are thus unable to explain the origin of this sequence as being due to self-excited pulsation. We speculate that these stars may have their fundamental mode excited by the phenomenon that generates the LSPs seen between sequences C and D. The origin of these LSPs, and the LSPs of sequence D, is unknown.

We thank W. A. Dziembowski for helpful comments. The research leading to these results has received funding from the European Research Council under the European Community's Seventh Framework Programme (FP7/2007-2013)/ERC grant agreement No. 246678. This work has been supported by the Polish National Science Centre grant No. DEC-2011/03/B/ST9/02573. P.R.W. acknowledges partial support provided by Australian Research Council Discovery Project DP120103337. He is also grateful for the hospitality provided by the Department of Astronomy, University of Padova, where much of his work on this paper was done.

REFERENCES

Cutri, R. M., Skrutskie, M. F., van Dyk, S., et al. 2003, 2MASS All Sky Catalog of Point Sources (Pasadena, CA: NASA/IPAC)
Fox, M. W., & Wood, P. R. 1982, ApJ, 259, 198
Fraser, O. J., Hawley, S. L., & Cook, K. H. 2008, AJ, 136, 1242
Glass, I. S., & Evans, T. L. 1981, Natur, 291, 303
Ita, Y., & Matsunaga, N. 2011, MNRAS, 412, 2345
Ita, Y., Tanabé, T., Matsunaga, N., et al. 2004, MNRAS, 347, 720
Kallinger, T., Mosser, B., Hekker, S., et al. 2010, A&A, 522, A1
Kamath, D., Wood, P. R., Soszyński, I., & Lebzelter, T. 2010, MNRAS, 408, 522
Keller, S. C., & Wood, P. R. 2006, ApJ, 642, 834
Kerschbaum, F., Lebzelter, T., & Lazaro, C. 2001, A&A, 375, 527
Kholopov, P. N., Samus, N. N., Kazarovets, E. V., & Perova, N. B. 1985–1988, in General Catalogue of Variable Stars (4th ed.; Moscow: Sternberg Astronomical Institute)
Kiss, L. L., & Bedding, T. R. 2003, MNRAS, 343, L79
Lebzelter, T., & Obbrugger, M. 2009, AN, 330, 390
Marigo, P., & Aringer, B. 2009, A&A, 508, 1539
Mosser, B., Belkacem, K., Goupil, M.-J., et al. 2010, A&A, 517, A22
Nicholls, C. P., Wood, P. R., & Cioni, M.-R. L. 2010, MNRAS, 405, 1770
Nicholls, C. P., Wood, P. R., Cioni, M.-R. L., & Soszyński, I. 2009, MNRAS, 399, 2063
Schlegel, D. J., Finkbeiner, D. P., & Davis, M. 1998, ApJ, 500, 525
Soszyński, I., Dziembowski, W. A., Udalski, A., et al. 2007, AcA, 57, 201
Soszyński, I., Udalski, A., Kubiak, M., et al. 2004a, AcA, 54, 129
Soszyński, I., Udalski, A., Kubiak, M., et al. 2004b, AcA, 54, 347
Soszyński, I., Udalski, A., Kubiak, M., et al. 2005, AcA, 55, 331
Soszyński, I., Udalski, A., Szymański, M. K., et al. 2009, AcA, 59, 239
Soszyński, I., Udalski, A., Szymański, M. K., et al. 2011, AcA, 61, 217
Stothers, R. B. 2010, ApJ, 725, 1170
Tabur, V., Bedding, T. R., Kiss, L. L., et al. 2010, MNRAS, 409, 777
Templeton, M. R., Mattei, J. A., & Willson, L. A. 2005, AJ, 130, 776
Udalski, A. 2003, AcA, 53, 291
Vassiliadis, E., & Wood, P. R. 1993, ApJ, 413, 641
Wood, P. R. 2000, PASA, 17, 18
Wood, P. R., Alcock, C., Allsman, R. A., et al. 1999, in IAU Symp. 191, Asymptotic Giant Branch Stars, ed. T. Le Bertre, A. Lebre, & C. Waelkens (Cambridge: Cambridge Univ. Press), 151
Wood, P. R., Bessell, M. S., & Fox, M. W. 1983, ApJ, 272, 99
Wood, P. R., Olivier, E. A., & Kawaler, S. D. 2004, ApJ, 604, 800
Wood, P. R., & Sebo, K. M. 1996, MNRAS, 282, 958
Wray, J. J., Eyer, L., & Paczyński, B. 2004, MNRAS, 349, 1059